Linear inversion of absorptive/dispersive wave field measurements: theory and 1D synthetic tests

Kristopher A. Innanen and Arthur B. Weglein

Abstract

The use of inverse scattering theory for the inversion of viscoacoustic wave field measurements, namely for a set of parameters that includes Q, is by its nature very different from most current approaches for Q estimation. In particular, it involves an analysis of the angle- and frequency-dependence of amplitudes of viscoacoustic data events, rather than the measurement of temporal changes in the spectral nature of events. We consider the linear inversion for these parameters theoretically and with synthetic tests. The output is expected to be useful in two ways: (1) on its own it provides an approximate distribution of Q with depth, and (2) higher order terms in the inverse scattering series as it would be developed for the viscoacoustic case would take the linear inverse as input.

We will begin, following Innanen (2003) by casting and manipulating the linear inversion problem to deal with absorption for a problem with arbitrary variation of wavespeed and Q in depth, given a single shot record as input. Having done this, we will numerically and analytically develop a simplified instance of the 1D problem. This simplified case will be instructive in a number of ways, first of all in demonstrating that this type of direct inversion technique relies on reflectivity, and has no interest in or ability to analyse propagation effects as a means to estimate Q. Secondly, through a set of examples of slightly increasing complexity, we will demonstrate how and where the linear approximation causes more than the usual levels of error. We show how these errors may be mitigated through use of specific frequencies in the input data, or, alternatively, through a layer-stripping based, or bootstrap, correction. In either case the linear results are encouraging, and suggest the viscoacoustic inverse Born approximation may have value as a standalone inversion procedure.

1 Introduction

A well-known and oft-mentioned truism in reflection seismic data processing is that, broadly put, the velocity structure of the subsurface impacts the recorded wave field in two important ways:

(1) rapid variations in Earth properties (such as velocity) give rise to reflection effects, and
(2) slow variations give rise to propagation effects (e.g. move-out etc.)

Wave theory predicts an exact parallel of this truism for the case of an absorptive/dispersive medium. That is,

(1) contrasts in absorptive/dispersive Earth parameters produce a characteristic reflectivity, and
(2) trends cause characteristic propagation effects, namely amplitude decay and dispersion.

In spite of this direct parallel, there is a striking discrepancy between the way seismic parameter inversion takes place in these two instances; acoustic/elastic inversion makes primary use of (1), via AVO-like methods, and absorptive/dispersive inversion makes use of (2), usually via the study of trends in amplitude decay for Q estimation. The reason for the discrepancy is entirely practical: for absorptive/dispersive media, the propagation effects of Q dominate over the reflectivity effects. It is certainly very sensible to make use of the dominant effects of a parameter in its estimation (see for instance Tonn, 1991; Dasgupta and Clark, 1998). Notwithstanding, permit us to make some comments negative to this approach.

First, a correction: of course, acoustic data processing *does* involve propagation-based inversion, in velocity analysis (but the output velocity field is not considered an end in itself). This will be an instructive analogy. Both propagation-based velocity analysis, and propagation-based Q-estimation, gain their effectiveness by evaluating changes that span the data set (in spatial and temporal domains), either by monitoring move-out or by monitoring ratios of spectral amplitudes. Estimating parameters by observing trends in the data set must be a somewhat *ad hoc* process, always requiring some level of assumption about the nature of the medium. Examples are so well-known as to be scarcely worth mentioning, but one thinks immediately of NMO-based velocity analysis, which in its most basic form requires a medium made up of horizontal layers. The difference between Q-estimation techniques and velocity analysis techniques is that the latter have been developed to states of great complexity and sophistication, such that many of these destructive assumptions are avoided (e.g., through techniques of reflection tomography). Comparatively, most Q estimation techniques are simple, often based on the assumption that there is a single Q value that dictates the absorptive behaviour of a wave field everywhere in the medium.

If we seriously think that the data we measure are shaped and altered by wave propagation that follows a known attenuation law, and if we want to be able to determine the medium parameters, including Q, badly enough to (a) take high quality data and (b) look at it very closely, then an increased level of sophistication is required.

An effort to usefully increase the level of sophistication of Q estimation can go one of two or more ways (we'll mention two), and this harkens back to the aforementioned discrepancy in inversion approaches. First, we could follow the development of propagation based inversion, or velocity analysis, towards a tomographic/ray tracing milieu in which local spectral characteristics of an event are permitted to be due to a Q that varies along the ray path, and a spatial distribution of Q is estimated along these lines. This could provide a useful, but smooth, spatial distribution of Q.

Second, we could make absorptive/dispersive inversion procedures more closely imitate their acoustic/elastic brethren, and focus rather on a close analysis of angle- and frequency-dependent amplitudes of data events. There are many reasons to shy away from this kind of approach, all of which stem from the idea of dominant effects – Q-like reflectivity is a lot less detectable than Q-like propagation.

The reasons in favour of the pursuit of such an inversion for absorptive/dispersive medium parameters likewise all stem from a single idea: the inverse scattering series demands that we do it that way. We listen to such demands because of the promise of the inverse scattering series: to provide a multidimensional reconstruction of the medium parameters that gave rise to the scattered wave field, with no assumptions about the structure of the medium, and no requirement of an accurate velocity model as input. Suppose we measure the scattered wave field above an absorptive/dispersive medium with sharp contrasts in Q as well as the wavespeed, and suppose we cast the inverse scattering series problem with an acoustic (non-attenuating) Green's function. First, since the series will reconstruct the sharp medium transitions from attenuated – smoothed – data, a *de facto* Q compensation must be occurring. Second, since Q is entirely within the perturbation (given an acoustic reference), the reconstruction is a *de facto* Q estimation. In other words, without dampening our spirits by considering issues of practical implementation, the viscoacoustic inverse scattering series must accomplish these two tasks, a multidimensional Q compensation and estimation, in the absence of an accurate foreknowledge of Q. It is this promise that motivates an investigation into the use of inverse scattering techniques to process and invert absorptive/dispersive wave field measurements.

The first step in doing so is to investigate the linear inversion problem, and it is to this component of the problem that the bulk of this paper is geared. The results of linear inversion are of course often tremendously useful on their own, and this is both true and untrue of the absorptive/dispersive case.

We will begin by casting and manipulating the linear inversion to deal with arbitrary variation of wavespeed and Q in depth, given a single shot record as input. Having done this, we will numerically and analytically develop a simplified instance of the 1D problem. This simplified case will be instructive in a number of ways, first of all in demonstrating that this type of direct inversion technique relies on reflectivity, and has no interest in or ability to analyze propagation effects as a means to estimate Q. Secondly, through a set of examples of slightly increasing complexity, we will demonstrate how and where the linear approximation causes more than the usual levels of error. We show how these errors may be mitigated through use of specific frequencies in the input data, or, alternatively, through a layer-stripping based, or bootstrap, correction. In either case the linear results are encouraging, and suggest the viscoacoustic Born approximation may have value as a standalone inversion procedure.

Obviously analysis of this kind relies heavily on correctly modelling the behaviour of the reflection coefficient at viscous boundaries. We give this important question short shrift here, by taking a well-known model for attenuation and swallowing it whole; and to be sure, the quality of the inversion results depend on the adequacy of these models to predict the behaviour of the viscous reflection coefficient. On the other hand, the frequency dependence of $R(f)$, which provides the information driving the inversion, is a consequence of contrasts in media with dispersive behaviour. All theory falls in line given the presence of a dispersive character in the medium, in principle if not in the detail of this chosen attenuation model.

2 Casting the Absorptive/Dispersive Problem

In acoustic/elastic/anelastic (etc.) wave theory, the parameters describing a medium are related non-linearly to the measurements of the wave field. Many forms of direct wave field inversion, including those used in this paper, involve a linearization of the problem, in other words a solution for those components of the model which are linear in the measured data.

There are two reasons for solving for the linear portion of the model. First, if the reference Green's function is sufficiently close to the true medium, then the linear portion of the model may be, in and of itself, of value as a close approximation to the true Earth. Second, a particular casting of the inverse scattering series uses this linear portion of the scattering potential (or model) as input for the solution of higher order terms. It is useful to bear in mind that the decay of the proximity of the Born inverse to the real Earth does not, in methods based on inverse scattering, signal the end of the utility of the output. Rather, it marks the start of the necessity for inclusion, if possible, of higher order terms – terms "beyond Born".

Seismic events are often better modelled as having been generated by changes in multiple Earth parameters than in a single one; for instance, density and wavespeed in an impedance-type description, or density and bulk modulus in a continuum mechanics-type description. In either case, the idea is that a single parameter velocity inversion (after that of Cohen and Bleistein (1977)) encounters problems because the amplitude of events is not reasonably explicable with a single parameter.

In Clayton and Stolt (1981) and Raz (1981), density/bulk modulus and density/wavespeed models respectively are used with a single-scatterer approximation to invert linearly for profiles of these parameters. In both cases it is the variability of the data in the offset dimension that provides the information necessary to separate the two parameters. The key (Clayton and Stolt, 1981; Weglein, 1985) is to arrive at a relationship between the data and the linear model components in which, for each instance of an experimental variable, an independent equation is produced. For instance, in an AVO type problem, an overdetermined system of linear equations is produced (one equation for each offset), which may be solved for multiple parameters.

In a physical problem involving dispersion, waves travel at different speeds depending on the frequency, which means that, at regions of sharp change of the inherent viscoacoustic properties of the medium, frequency-dependent reflection coefficients are found. This suggests that one might look to the frequency content of the data as a means to similarly separate some appropriately-chosen viscoacoustic parameters (i.e. wavespeed and Q).

We proceed by adopting a Q model similar to those discussed by Aki and Richards (2002) and equivalent to that of Kjartansson (1979) under certain assumptions, such that the dispersion relation is assumed, over a reasonable seismic bandwidth, to be given by

$$k(z) = \frac{\omega}{c(z)}\left[1 + \frac{i}{2Q(z)} - \frac{1}{\pi Q(z)}\ln\left(\frac{k}{k_r}\right)\right], \tag{1}$$

where $k_r = \omega_r/c_0$ is a reference wavenumber, $k = \omega/c_0$, and where c_0 is a reference wavespeed to be discussed presently. As discussed previously, this specific choice of Q model is crucial to the mathematical detail of what is to follow; however we consider the general properties of the inverse method we develop to be well geared to handle the general properties of the Q model.

This is re-writeable using an attenuation parameter $\beta(z) = 1/Q(z)$ multiplied by a function $F(k)$, of known form:

$$F(k) = \frac{i}{2} - \frac{1}{\pi}\ln\left(\frac{k}{k_r}\right), \tag{2}$$

which utilizes $\beta(z)$ to correctly instill both the attenuation ($i/2$) and dispersion ($-\frac{1}{\pi}\ln(k/k_r)$). Notice that $F(k)$ is frequency-dependent because of the dispersion term. Then

$$k(z) = \frac{\omega}{c(z)}\left[1 + \beta(z)F(k)\right]. \tag{3}$$

The linearized Born inversion is based on a choice for the form of the scattering potential V, which is given by

$$\mathbf{V} = \mathbf{L} - \mathbf{L}_0, \tag{4}$$

or the difference of the wave operators describing propagation in the reference medium ($\mathbf{L}_0$) and the true medium ($\mathbf{L}$). For a constant density medium with a homogeneous reference this amounts to

$$\mathbf{V} = V(x,z,k) = k^2(x,z) - \frac{\omega^2}{c_0^2}, \tag{5}$$

for a medium which varies in two dimensions, or

$$V(z,k) = k^2(z) - \frac{\omega^2}{c_0^2}, \tag{6}$$

for a 1D profile. Using equation (3), we specify the wavespeed/Q scattering potential to be

$$V(x,z,k) = \frac{\omega^2}{c^2(x,z)}\left[1 + \beta(x,z)F(k)\right]^2 - \frac{\omega^2}{c_0^2}, \tag{7}$$

and include the standard perturbation on the wavespeed profile $c(x,z)$ in terms of $\alpha(x,z)$ and a reference wavespeed c_0, producing

$$\begin{aligned} V(x,z,k) &= \frac{\omega^2}{c_0^2}[1-\alpha(x,z)]\,[1+\beta(x,z)F(k)]^2 - \frac{\omega^2}{c_0^2} \\ &\approx -\frac{\omega^2}{c_0^2}[\alpha(x,z) - 2\beta(x,z)F(k)], \end{aligned} \tag{8}$$

dropping all terms quadratic and higher in the perturbations α and β. The 1D profile version of this scattering potential is then, straightforwardly

$$V(z,k) \approx -\frac{\omega^2}{c_0^2}[\alpha(z) - 2\beta(z)F(k)]. \tag{9}$$

The scattering potential in equation (9) will be used regularly in this paper.

3 Inversion for Q/Wavespeed Variations in Depth

The estimation of the 1D contrast (i.e. in depth) of multiple parameters from seismic reflection data is considered, similar to, for instance, Clayton and Stolt (1981). For the sake of exposition we demonstrate how the problem is given the simplicity of a normal-incidence experiment by considering the bilinear form of the Green's function. In 1D, for instance, the Green's function, which has the nominal form

$$G_0(z_g|z';\omega) = \frac{e^{ik|z_g - z'|}}{2ik}, \tag{10}$$

also has the bilinear form

$$G_0(z_g|z';\omega) = \frac{1}{2\pi}\int_{-\infty}^{\infty} dk'_z \frac{e^{ik'_z(z_g - z')}}{k^2 - {k'_z}^2}, \tag{11}$$

where $k = \omega/c_0$. Consider the reference medium to be acoustic with constant wavespeed c_0. The scattered wave field (measured at x_g, z_g for a source at x_s, z_s), $\psi_s(x_g, z_g|x_s, z_s;\omega)$, is related to model components that are linear in the data; these are denoted $V_1(z,\omega)$. This relationship is given by the exact equation

$$\psi_s(x_g,z_g|x_s,z_s;\omega) = S(\omega)\int_{-\infty}^{\infty} dx' \int_{-\infty}^{\infty} dz' G_0(x_g,z_g|x',z';\omega)V_1(z',\omega)G_0(x',z'|x_s,z_s;\omega) \tag{12}$$

where S is the source waveform. The function G_0 describes propagation in the acoustic reference medium, and can be written as a 2D Green's function in bilinear form:

$$G_0(x_g, z_g|x', z'; \omega) = \frac{1}{(2\pi)^2} \int_{-\infty}^{\infty} dk'_x \int_{-\infty}^{\infty} dk'_z \frac{e^{ik'_x(x_g-x')} e^{ik'_z(z_g-z')}}{k^2 - ({k'_x}^2 + {k'_z}^2)}, \tag{13}$$

where $k = \omega/c_0$. Measurements over a range of x_g will permit a Fourier transform to the coordinate k_{xg} in the scattered wave field. On the right hand side of equation (12) this amounts to taking the Fourier transform of the left Green's function $G_0(x_g, z_g|x', z'; \omega)$:

$$G_0(k_{xg}, z_g|x', z'; \omega) = \frac{1}{(2\pi)^2} \int_{-\infty}^{\infty} dk'_x \int_{-\infty}^{\infty} dk'_z \int_{-\infty}^{\infty} dx_g \frac{e^{-ik_{xg}x_g} e^{ik'_x(x_g-x')} e^{ik'_z(z_g-z')}}{k^2 - ({k'_x}^2 + {k'_z}^2)}. \tag{14}$$

Taking advantage of the sifting property of the Fourier transform:

$$\begin{aligned}
G_0(k_{xg}, z_g|x', z'; \omega) &= \frac{1}{(2\pi)^2} \int_{-\infty}^{\infty} dk'_x \int_{-\infty}^{\infty} dk'_z \int_{-\infty}^{\infty} dx_g \frac{e^{i(k_{xg}-k'_m)x_g} e^{-ik'_x x'} e^{ik'_z(z_g-z')}}{k^2 - ({k'_x}^2 + {k'_z}^2)} \\
&= \frac{1}{(2\pi)^2} \int_{-\infty}^{\infty} dk'_x \int_{-\infty}^{\infty} dk'_z \frac{e^{-ik'_x x'} e^{ik'_z(z_g-z')}}{k^2 - ({k'_x}^2 + {k'_z}^2)} \left[\int_{-\infty}^{\infty} dx_g e^{i(k_{xg}-k'_m)x_g} \right] \\
&= \frac{1}{2\pi} \int_{-\infty}^{\infty} dk'_x \int_{-\infty}^{\infty} dk'_z \frac{e^{-ik'_x x'} e^{ik'_z(z_g-z')}}{k^2 - ({k'_x}^2 + {k'_z}^2)} \delta(k'_x - k_{xg}) \\
&= \frac{1}{2\pi} e^{-ik_{xg}x'} \int_{-\infty}^{\infty} dk'_z \frac{e^{ik'_z(z_g-z')}}{q_z^2 + {k'_z}^2},
\end{aligned} \tag{15}$$

where $q_z^2 = k^2 - {k_{xg}}^2$, a vertical wavenumber. Notice that the remaining integral is a 1D Green's function in bilinear form, as in equation (11). So equation (15) takes on the remarkably simplified form:

$$G_0(k_{xg}, z_g|x', z'; \omega) = e^{-ik_{xg}x'} \left[\frac{e^{iq_z|z_g-z'|}}{2iq_z} \right]. \tag{16}$$

The righthand Green's function in equation (12) may likewise be written

$$G_0(x', z'|x_s, z_s; \omega) = \frac{1}{(2\pi)^2} \int_{-\infty}^{\infty} dk_{xs} \int_{-\infty}^{\infty} dk_{zs} \frac{e^{ik_{xs}(x'-x_s)} e^{ik_{zs}(z'-z_s)}}{k^2 - ({k_{xs}}^2 + {k_{zs}}^2)}, \tag{17}$$

and therefore the scattered wave field becomes

$$\begin{aligned}
\psi_s(k_{xg}, z_g|x_s, z_s; \omega) =& S(\omega) \frac{1}{(2\pi)^2} \int_{-\infty}^{\infty} dx' \int_{-\infty}^{\infty} dz' e^{-ik_{xg}x'} \frac{e^{iq_z|z_g-z'|}}{2iq_z} \times \\
& \int_{-\infty}^{\infty} dk_{xs} \int_{-\infty}^{\infty} dk_{zs} \frac{e^{ik_{xs}(x'-x_s)} e^{ik_{zs}(z'-z_s)}}{k^2 - ({k_{xs}}^2 + {k_{zs}}^2)} V_1(z', \omega).
\end{aligned} \tag{18}$$

The seismic experiment is conducted along a surface, which for convenience may be set at $z_s = z_g = 0$. Further, since the subsurface being considered has variation in z only, all "shot-record" type experiments are identical, and only one need be considered. We let this one shot be at $x_s = 0$. This produces the simplified expression

$$\begin{aligned}\psi_s(k_{xg},0|0,0;\omega) =& S(\omega)\frac{1}{(2\pi)^2}\int_{-\infty}^{\infty}dx'\int_{-\infty}^{\infty}dz'\int_{-\infty}^{\infty}dk_{xs}\int_{-\infty}^{\infty}dk_{zs}\frac{e^{iq_z z'}}{2iq_z}\times \\ &\frac{e^{ik_{zs}z'}}{k^2-({k_{xs}}^2+{k_{zs}}^2)}e^{i(k_{xs}-k_{xg})x'}V_1(z',\omega),\end{aligned} \tag{19}$$

which, similarly to equation (15), becomes

$$\begin{aligned}\psi_s(k_{xg},0|0,0;\omega) &= S(\omega)\frac{1}{2\pi}\int_{-\infty}^{\infty}dz'\int_{-\infty}^{\infty}dk_{xs}\int_{-\infty}^{\infty}dk_{zs}\frac{e^{iq_z z'}}{2iq_z}\frac{e^{ik_{zs}z'}}{k^2-({k_{xs}}^2+{k_{zs}}^2)}\delta(k_{xs}-k_{xg})V_1(z',\omega) \\ &= S(\omega)\frac{1}{2\pi}\int_{-\infty}^{\infty}dz'\int_{-\infty}^{\infty}dk_{zs}\frac{e^{iq_z z'}}{2iq_z}\frac{e^{ik_{zs}z'}}{k^2-({k_{xg}}^2+{k_{zs}}^2)}V_1(z',\omega) \\ &= S(\omega)\frac{1}{2\pi}\int_{-\infty}^{\infty}dz'\frac{e^{iq_z z'}}{2iq_z}V_1(z',\omega)\left[\int_{-\infty}^{\infty}dk_{zs}\frac{e^{ik_{zs}z'}}{q_z^2+{k_{zs}}^2}\right],\end{aligned} \tag{20}$$

where again the vertical wavenumber $q_z^2 = k^2 - k_{xg}^2$ appears. The integral over dk_{zs} has the form of a 1D Green's function. The data equations (one for each frequency), with the choice $z_s = z_g = x_s = 0$, are now

$$\begin{aligned}\psi_s(k_{xg};\omega) &= S(\omega)\int_{-\infty}^{\infty}dz'\frac{e^{iq_z z'}}{2iq_z}V_1(z',\omega)\frac{e^{iq_z z'}}{2iq_z} \\ &= -\frac{S(\omega)}{4q_z^2}\int_{-\infty}^{\infty}dz' e^{i2q_z z'}V_1(z',\omega) \\ &= -\frac{S(\omega)}{4q_z^2}V_1(-2q_z,\omega),\end{aligned} \tag{21}$$

recognizing that the last integral is a Fourier transform of the scattering potential V_1. Thus one has an expression of the unknown perturbation V_1 (i.e. the model) that is linear in the data. Multiple parameters within V_1 may be solved if, frequency by frequency, the data equations (21) are independent.

Estimation of multiple parameters from data with offset (i.e. using AVO) requires that equations (21) be independent offset to offset. In the case of viscoacoustic inversion, we show that it is the dispersive nature of an attenuation model which produces the independence of the data equations with offset, allowing the procedure to go forward.

Consider the term $F(k)$:

$$F(k) = \frac{i}{2} - \frac{1}{\pi} \ln\left(\frac{k}{k_r}\right). \tag{22}$$

As mentioned, the frequency dependence of F arises from the rightmost component in equation (22), the dispersion component. In 1D wave propagation, this amounts to the "rule" by which the speed of the wave field alters, frequency by frequency, with respect to the reference wavenumber $k_r = \omega_r/c_0$, usually chosen using the largest frequency of the seismic experiment. In 2D wave propagation, F, which changes the propagation wavenumber $k(z)$ in equation (3), now alters the wave field along its direction of propagation in (x, z). Let θ represent the angle away from the downward, positive, z axis. A vertical wavenumber q_z is related to k by $q_z = k\cos\theta$; if one replaces the reference wavenumber k_r with a reference angle θ_r and reference vertical wavenumber q_{zr}, then F becomes

$$\begin{aligned} F(k) &= \frac{i}{2} - \frac{1}{\pi} \ln\left(\frac{k}{k_r}\right) \\ &= \frac{i}{2} - \frac{1}{\pi} \ln\left(\frac{q_z \cos\theta_r}{q_{zr}\cos\theta}\right). \end{aligned} \tag{23}$$

Then:

$$F(\theta, q_z) = \frac{i}{2} - \frac{1}{\pi} \ln\left(\frac{q_z \cos\theta_r}{q_{zr}\cos\theta}\right), \tag{24}$$

so what remains is a function which, for a given vertical wavenumber, predicts an angle dependent alteration to the wave propagation. As such the scattering potential may be written as a function of angle and vertical wavenumber also:

$$V(z, \theta, q_z) = -\frac{\omega^2}{c_0^2}[\alpha(z) - 2\beta(z)F(\theta, q_z)]. \tag{25}$$

The angle dependence of F produces independent sets of data equations, since it alters the coefficient of $\beta(z)$ for different angles while leaving $\alpha(z)$ untouched. Using equation (25), one may write the linear component of a depth-dependent only scattering potential as:

$$V_1(z, \theta, q_z) = -\frac{\omega^2}{c_0^2}[\alpha_1(z) - 2\beta_1(z)F(\theta, q_z)]. \tag{26}$$

Recall from earlier in this section that the requisite data equations are

$$\psi_s(k_{xg}; \omega) = -\frac{S(\omega)}{4q_z^2} V_1(-2q_z, \omega); \tag{27}$$

using equation (26), and considering the surface expression of the wave field to be the data, deconvolved of $S(\omega)$, this becomes

$$D(q_z,\theta) = K_1(\theta)\alpha_1(-2q_z) + K_2(\theta,q_z)\beta_1(-2q_z), \tag{28}$$

where

$$K_1(\theta) = \frac{1}{4\cos^2\theta}, \qquad K_2(\theta,q_z) = -2\frac{F(\theta,q_z)}{4\cos^2\theta}. \tag{29}$$

Notice that in equation (29) we have more than one equation at each wavenumber q_z; every offset or angle θ provides an independent equation, and so in an experiment with many offsets we have an overdetermined problem.

4 A Complex, Frequency Dependent Reflection Coefficient

The success of such an attempt to extract linear viscoacoustic perturbations as above is obviously, therefore, contingent on detecting the impact of the frequency-dependent viscoacoustic reflection coefficient $R(k)$ on the data amplitudes. This is an important aspect of a scattering-based attempt to process and invert seismic data taking such lossy propagation into account: the inverse scattering series will look to the frequency- and angle-dependent aspects of the measured events for information on Q.

Using previously-defined terminology, the reflection coefficient for an 1D acoustic wave field normally incident on a contrast in wavespeed (from c_0 to c_1) and Q (from ∞ to Q_1), is

$$R(k) = \frac{1 - \frac{c_0}{c_1}\left(1 + \frac{F(k)}{Q_1}\right)}{1 + \frac{c_0}{c_1}\left(1 + \frac{F(k)}{Q_1}\right)}. \tag{30}$$

This is a complex, frequency[1] dependent quantity that will alter the amplitude and phase spectra of the measured wave field. The spectra of reflection coefficients of this form for a single wavespeed contrast ($c_0 = 1500$m/s to $c_1 = 1600$m/s) and a variety of Q_1 values is illustrated in Figure 1. The attenuative reflection coefficient approaches its acoustic counterpart as $Q_1 \to \infty$; the variability of R with f increases away from the reference wavenumber. Equation (1), and hence equation (30), relies on $\left|\frac{1}{Q_1}\ln\left(\frac{f}{f_r}\right)\right| \ll 1$, and so at low frequency we must consider the accuracy of the current Q model. But a problematic $\ln(f/f_r) \approx -Q_1$ requires $f/f_r \approx e^{-Q_1}$, which keeps us out of trouble for almost all realistic combinations of f and Q, with the exception of the very lowest frequencies.

[1] We sometimes refer to wavenumbers k_1 and k_2 as "frequencies", referring to the simple relationship with f as in $k_1 = 2\pi f_1/c_0$. Also, usefully, ratios of frequency-related quantities are equivalent: $f/f_r = \omega/\omega_r = k/k_r$.

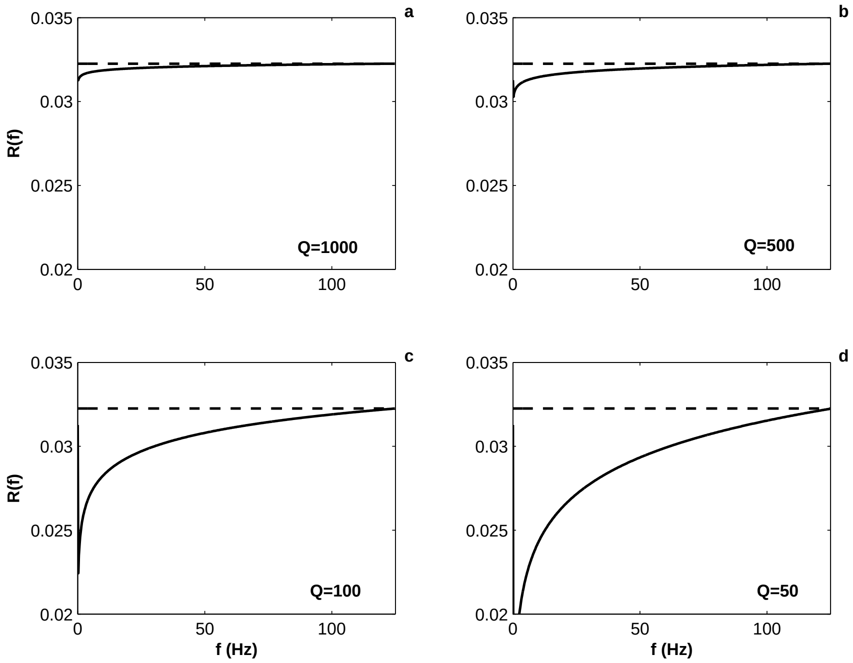

Figure 1*: Real component of the reflection coefficient* $R(f)$*, where* $f = kc_0/2\pi$*, over the frequency interval associated with a* $4s$ *experiment with* $\Delta t = 0.004s$*, and a reference frequency of* $k_r c_0/2\pi = f_r = 125Hz$*. The acoustic (non-attenuating) reflection coefficient* $R' = (c_0 - c_1)/(c_0 + c_1)$ *is included as a dashed line.* Q_1 *values are (a)* 1000*, (b)* 500*, (c)* 100*, and (d)* 50*.*

5 Analytic/Numeric Tests: The 1D Normal Incidence Problem

In general it is not possible to invert for two parameters from a 1D normal incidence seismic experiment. However, if one assumes a basic spatial form for the Earth model (or perturbation from reference model), then this problem becomes tractable for a dispersive Earth. The discussion in this section continues along these lines, i.e. diverging from the more general inversion formalism developed previously. In doing so, it benefits from the simplicity of the 1D normal incidence example: many key features of the "normal incidence + structural assumptions" problem are shared by the "offset + no structural assumptions" problem, but the former are easier to compute and analyze.

Consider an experiment with coincident source and receiver $z_s = z_g = 0$. The linear data equation, in which the data are assumed to be the scattered field ψ_s measured at this source/receiver point, is

$$D(k) = \psi_s(0|0;k) = \int_{-\infty}^{\infty} G_0(0|z';k)k^2\gamma_1(z')\psi_0(z'|0;k)dz', \tag{31}$$

which, following the substitution of the acoustic 1D homogeneous Green's function and plane wave expressions G_0 and ψ_0 becomes

$$D(k) = -\frac{1}{2} ik\gamma_1(-2k), \tag{32}$$

where the integral is recognized as being a Fourier transform of the linear portion of the perturbation, called $\gamma_1(z)$. The form for the perturbation is given by the difference between the wave operators for the reference medium ($\mathbf{L}_0$) and the non-reference medium ($\mathbf{L}$), as discussed above. In this case, let the full scattering potential be due to a perturbation γ:

$$\gamma(z) = \frac{V(z,k)}{k^2}, \tag{33}$$

where $V(z,k)$ is given by equation (9). Writing the linear portion of the overall perturbation as

$$\gamma_1(z) = 2\beta_1(z)F(k) - \alpha_1(z), \tag{34}$$

taking its Fourier transform, and inserting it into equation (32), the data equations

$$D(k) = -\frac{1}{2} ik[2\beta_1(-2k)F(k) - \alpha_1(-2k)], \tag{35}$$

or

$$\alpha_1(-2k) - 2\beta_1(-2k)F(k) = 4\frac{D(k)}{i2k} \tag{36}$$

are produced.

Equation (36) as it stands cannot be used to separate α_1 and β_1. This is because at every wavenumber one has a single equation and two unknowns. However, much of the information garnered from the data, frequency by frequency, is concerned with determining the spatial distribution of these parameters. If a specific spatial dependence is imposed on α_1 and β_1 the situation is different.

Consider a constant density acoustic reference medium (a 1D homogeneous whole space) characterized by wavespeed c_0; let it be perturbed by a homogeneous viscoacoustic half-space, characterized by the wavespeed c_1, and now also by the Q-factor Q_1. The contrast occurs at $z = z_1 > 0$. Physically, this configuration amounts to probing a step-like interface with a normal incidence wave field, in which the medium above the interface (i.e. the acoustic overburden) is known. This is illustrated in Figure 2.

Data from an experiment over such a configuration are measurements of a wave field event that has a delay of $2z_1/c_0$ and that is weighted by a complex, frequency dependent reflection coefficient:

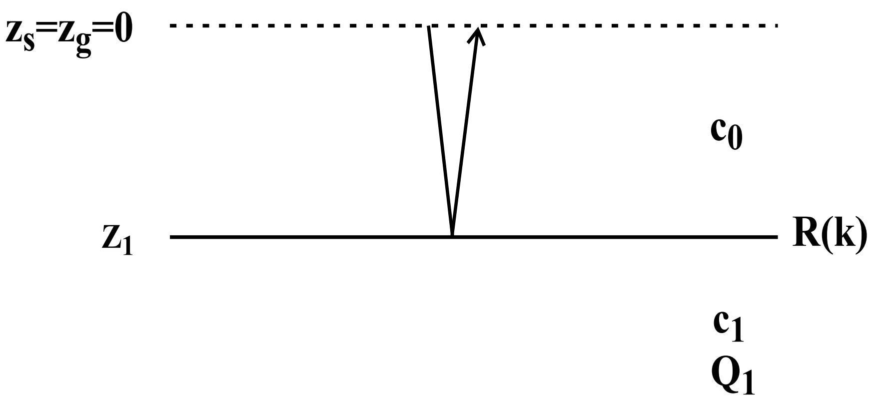

Figure 2: *Single interface experiment involving a contrast in wavespeed c_0 and Q.*

$$D(k) = R(k)e^{i2kz_1}. \tag{37}$$

This may be equated to the right-hand side of equation (35), in which the perturbation parameters are given the spatial form of a Heaviside function with a step at z_1. This is the pseudo-depth, or the depth associated with the reference wavespeed c_0 and the measured arrival time of the reflection. The data equations become

$$R(k)e^{i2kz_1} = \frac{1}{2}ik\left[\alpha_1\frac{e^{i2kz_1}}{i2k} - 2\beta_1\frac{e^{i2kz_1}}{i2k}F(k)\right], \tag{38}$$

or

$$\alpha_1 - 2\beta_1 F(k) = 4R(k), \tag{39}$$

in which α_1 and β_1 are constants. So having assumed a spatial form for the perturbations, the data equations (39) are now overdetermined, with two unknowns and as many equations as there are frequencies in the experiment. Notice that it is the frequency dependence of $F(k)$ that ensures these equations are independent – hence, it is the dispersive nature of the attenuative medium that permits the inversion to take place.

In an experiment with some reasonable bandwidth, the above relationship constitutes an overdetermined problem. If the reflection coefficient at each of N available frequencies ω_n (in which we label $k_n = \omega_n/c_0$) are the elements of a column vector $\mathbf{R}$, the unknowns α_1 and β_1 are the elements of a two-point column vector $\bar{\gamma}$, and we further define a matrix $\mathbf{F}$, such that:

$$\mathbf{R} = 4\begin{bmatrix} R(k_1) \\ R(k_2) \\ R(k_3) \\ \vdots \\ R(k_N) \end{bmatrix}, \quad \bar{\gamma} = \begin{bmatrix} \alpha_1 \\ \beta_1 \end{bmatrix}, \quad \text{and} \quad \mathbf{F} = \begin{bmatrix} 1 & -2F(k_1) \\ 1 & -2F(k_2) \\ 1 & -2F(k_3) \\ \vdots & \vdots \\ 1 & -2F(k_N) \end{bmatrix}, \tag{40}$$

then the relationship suggested by equation (39) is given by

$$\mathbf{F}\bar{\gamma} = \mathbf{R}. \tag{41}$$

Clearly then a solution to this problem involves computation of some approximation $\tilde{\bar{\gamma}} = \tilde{\mathbf{F}}^{-1}\mathbf{R}$; a least-squares approach is the most obvious.

The 1D normal incidence parameter estimation associated with the inversion of equation (39) is numerically illustrated below, firstly to show how well it works, and secondly to show how poorly it works. Following that we will respond to the latter aspect.

5.1 Numeric Examples I: Single Interface

We have a linear set of equations, one for each instance of available wavenumbers k_1, k_2, ...

$$\begin{aligned} &\alpha_1 - 2\beta_1 F(k_1) = 4R(k_1), \\ &\alpha_1 - 2\beta_1 F(k_2) = 4R(k_2), \\ &\alpha_1 - 2\beta_1 F(k_3) = 4R(k_3), \\ &\vdots \end{aligned} \tag{42}$$

In fact, estimating α_1 and β_1 is precisely equivalent to estimating (respectively) the y-intercept and slope of a set of data along the axes $4R(k)$ and $-2F(k)$. And similarly to the fitting of a line, provided we have perfect data we only require two input wavenumbers to get an answer. Letting these be $k_1 = \omega_1/c_0$ and $k_2 = \omega_2/c_0$, we may solve for estimates of $\alpha_1(k_1, k_2)$ and $\beta_1(k_1, k_2)$ for any pair of $k_1 \neq k_2$:

$$\begin{aligned} \beta_1(k_1, k_2) &= 2\frac{R(k_2) - R(k_1)}{F(k_1) - F(k_2)}, \\ \alpha_1(k_1, k_2) &= 4\frac{R(k_2)F(k_1) - R(k_1)F(k_2)}{F(k_1) - F(k_2)}. \end{aligned} \tag{43}$$

Equation (43) may be used along with a chosen Earth model to numerically test the efficacy of this inversion. Table 1 contains the details of four models:

Model	*Reference c_0 (m/s)*	*Non-reference c_1 (m/s)*	*Non-reference Q_1*
1	1500	1800	100
2	1500	1800	10
3	1500	2500	100
4	1500	2500	10

Table 1*: Test models used for the single interface c, Q linear inversion.*

Figures 3 – 6 show sets of recovered parameters using the respective models in Table 1. For the sake of illustration, frequency pairs $k_1 = k_2$, for which the inversion equations are singular, are smoothed using averages of adjacent ($k_1 \neq k_2$) results. The recovered Q values from the the measured viscoacoustic wave field are in error on the order of %1; this is true for all realistic contrasts in Q (i.e., up to $Q = 10$ as tested here). As the wavespeed contrast increases, the recovered Q is in greater error, but even in the large contrast cases of Models 3 and 4, the error is under %10. In all cases the error increases at low frequency; it is particularly acute when both k_1 and $k_2 \rightarrow 0$. The viscous linear inverse problem involves reflection coefficients that vary with frequency, in other words the "contrast" of the model is also effectively frequency-dependent. In a linear inversion, a frequency-dependent contrast implies a frequency-dependent accuracy level. It is encouraging to see that elsewhere, i.e. at larger k_1, k_2, the nominal acoustic (non-attenuating) Born approximation for the wavespeed is attained. Compare the results of Figure 3 (Model 1), for instance, with the 1D acoustic Born approximation associated with a wavespeed contrast of 1500m/s to 1800m/s (in which $R_1 \approx 0.091$):

$$c_1 \approx \frac{c_0}{(1-\alpha_1)^{1/2}}\text{m/s} = \frac{c_0}{(1-4R_1)^{1/2}}\text{m/s} \approx 1880.3\text{m/s}. \tag{44}$$

Since the wavespeed inversion results are very similar to those of a linear Born inversion in the absence of a viscous component, and the Q estimates are within a few percent of the correct value even at the highest reasonable contrast, we may declare this linear inversion example a success.

It has been noted elsewhere that linear Born inversion results tend to worsen in the presence of an unknown overburden, because of unaccounted-for transmission effects. Qualitatively, we might expect the absorptive/dispersive case to suffer greatly from this problem because of the exaggerated transmission effects of the lossy medium on the wave field amplitudes. In other words, if we add a second interface to the model, inversion error can be expected to worsen. Let us next gauge the extent of this error.

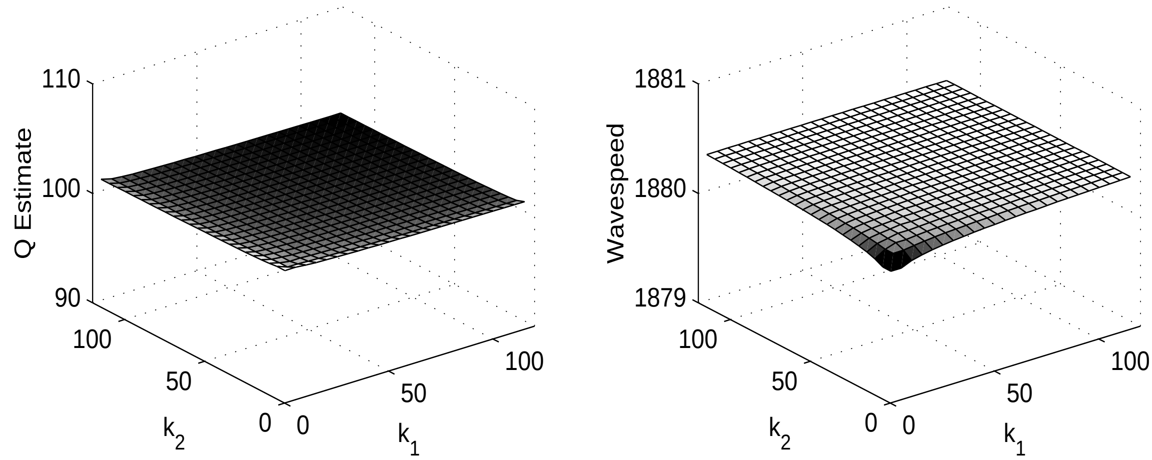

Figure 3*: Recovered parameters from the normal incidence linearized Born inversion for Q and wavespeed. Left: Q recovery using two (complex) reflection coefficients over a range of frequencies, k_1 and k_2 (Hz). Right: wavespeed recovery utilizing same (complex) reflection coefficients. Model parameters correspond to Model* 1 *in Table 1.*

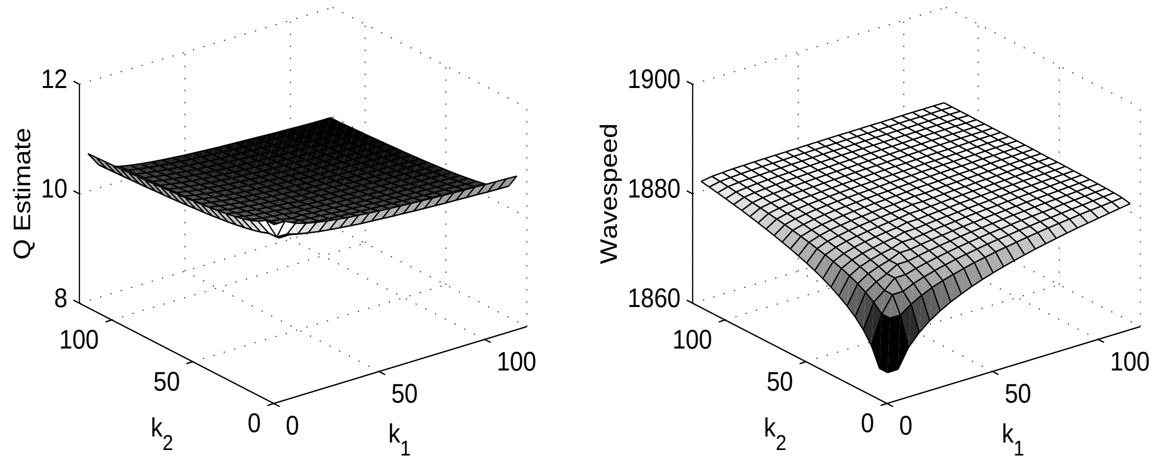

Figure 4*: Recovered parameters from the normal incidence linearized Born inversion for Q and wavespeed. Left: Q recovery using two (complex) reflection coefficients over a range of frequencies, k_1 and k_2 (Hz). Right: wavespeed recovery utilizing same (complex) reflection coefficients. Model parameters correspond to Model* 2 *in Table 1.*

5.2 Numeric Examples II: Interval Q Estimation

In a single parameter normal incidence problem, i.e. in which acoustic wavespeed contrasts are linearly inverted for from the data by trace integration, *profiles* may be generated, not just a single interface contrast. A similar procedure may be developed for the 1D normal incidence two parameter problem ($c(z)$ and $Q(z)$). We use the following model to describe

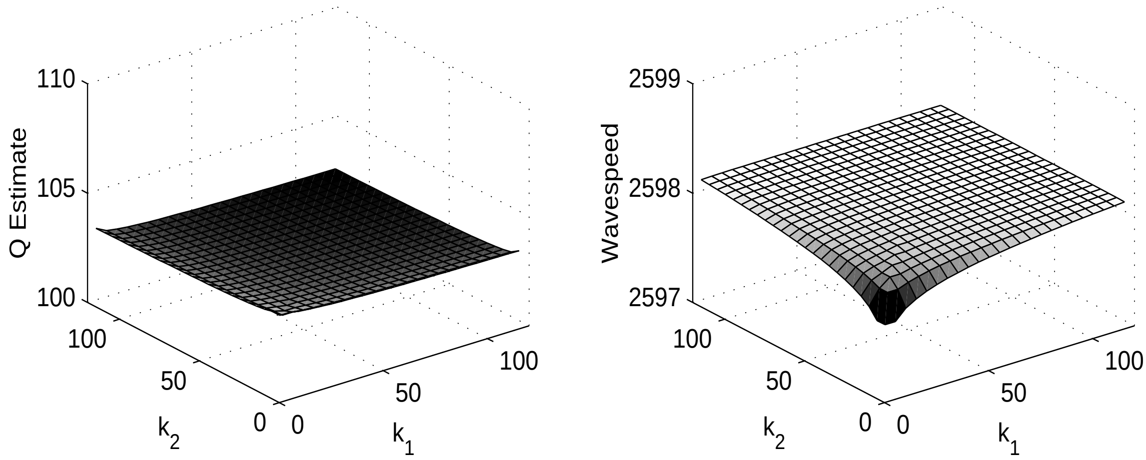

Figure 5*: Recovered parameters from the normal incidence linearized Born inversion for Q and wavespeed. Left: Q recovery using two (complex) reflection coefficients over a range of frequencies, k_1 and k_2 (Hz). Right: wavespeed recovery utilizing same (complex) reflection coefficients. Model parameters correspond to Model* 3 *in Table 1.*

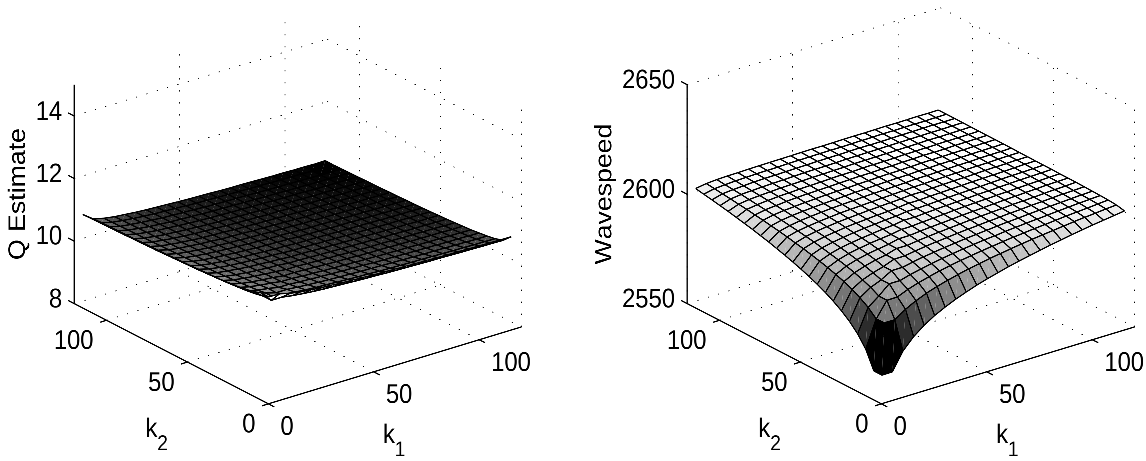

Figure 6*: Recovered parameters from the normal incidence linearized Born inversion for Q and wavespeed. Left: Q recovery using two (complex) reflection coefficients over a range of frequencies, k_1 and k_2 (Hz). Right: wavespeed recovery utilizing same (complex) reflection coefficients. Model parameters correspond to Model* 4 *in Table 1.*

the 1D normal incidence data associated with a model with N interfaces, at each of which the wavespeed and Q values are assumed to alter. The data are

$$D(k) = \sum_{n=1}^{N} D_n(k), \tag{45}$$

such that

$$\begin{aligned}
D_n(k) &= R'_n(k) \exp\left\{\sum_{j=1}^{n} i2k_{(j-1)}(z'_j - z'_{j-1})\right\}, \\
R'_n(k) &= R_n(k) \prod_{j=1}^{n-1}[1 - R_j^2(k)], \\
k_{(j)} &= \frac{\omega}{c_j}\left[1 + \frac{i}{2Q_j} - \frac{1}{\pi Q_j}\left(\frac{k}{k_r}\right)\right],
\end{aligned} \tag{46}$$

where, as ever, k is the acoustic reference wavenumber ω/c_0, and where $R_n(k)$ is the reflection coefficient of the n'th interface. The variables z'_j are the true depths of the interfaces. The exponential functions imply an arrival time and a "shape" for each event. Figure 7 shows an example data set of the form of equation (47) for a two-interface case in the conjugate (pseudo-depth) domain, i.e., in which

$$\begin{aligned}
D(k) &= D_1(k) + D_2(k) \\
&= R_1(k)e^{i2kz'_1} + R'_2(k)e^{i2kz_1}e^{i2k_{(1)}(z'_2 - z'_1)}.
\end{aligned} \tag{47}$$

Interpreting the data in terms of the acoustic reference wavespeed c_0, and with no knowledge of $Q(z)$, equation (47) becomes

$$D(k) = R_1(k)e^{i2kz_1} + \tilde{R}_2(k)e^{i2kz_1}e^{i2k(z_2 - z_1)}, \tag{48}$$

where z_j are pseudo-depths. Comparing equations (47) and (48), clearly the apparent reflection coefficient $\tilde{R}_2(k)$ has a lot to account for in the absorptive/dispersive case – not just the transmission coefficients $(1 - R_1^2(k))$, but now the attenuation as well. This is where the linear approximation is expected to encounter difficulty.

To pose the new interval Q problem, the total perturbations are written as the sum of the perturbations associated with each of these two events:

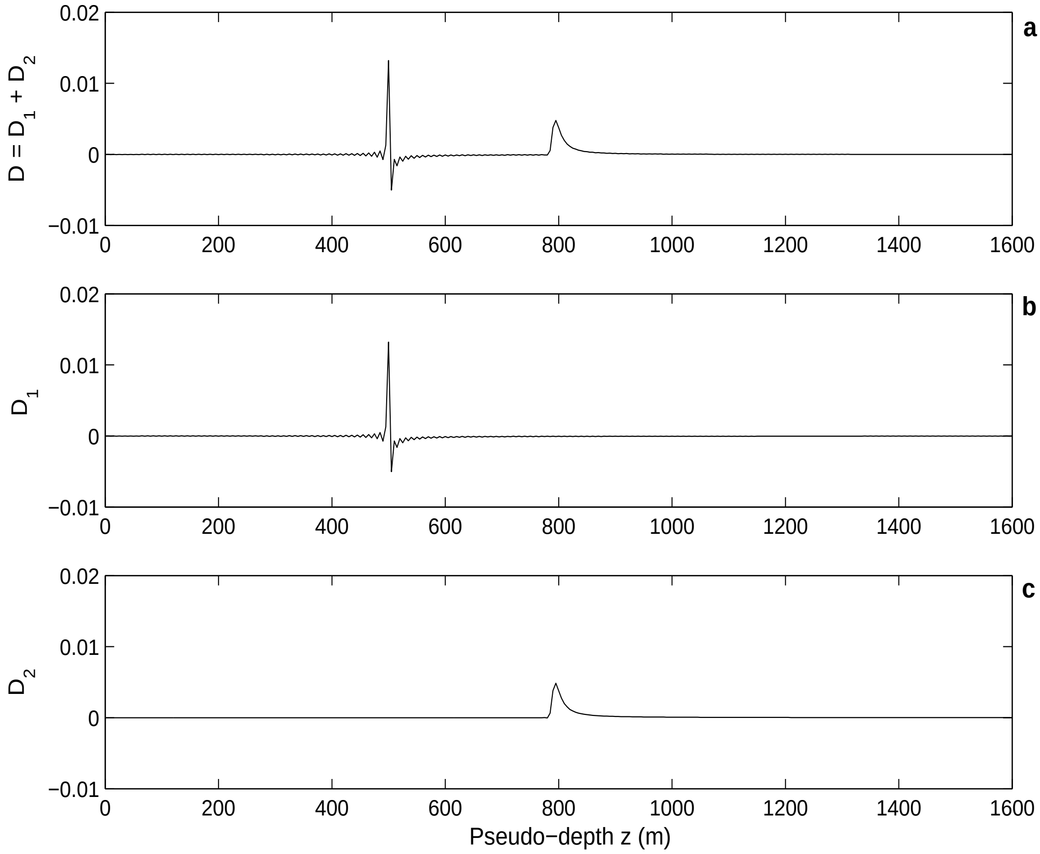

Figure 7: *Example data set of the type used to validate/demonstrate the linearized c, Q profile inversion. (a) Full synthetic trace, consisting of two events, $D_1 + D_2$, plotted in the conjugate (pseudo-depth) domain. The first event corresponds to the contrast from acoustic reference medium to a viscoacoustic layer, and the second corresponds to a deeper viscoacoustic contrast; (b) first event D_1 (plotted in the conjugate domain); (c) second event D_2.*

$$\begin{aligned}\alpha_1(-2k) &= \alpha_{11}(-2k) + \alpha_{12}(-2k)\\ \beta_1(-2k) &= \beta_{11}(-2k) + \beta_{12}(-2k),\end{aligned} \tag{49}$$

in which α_{1n}, β_{1n} are the perturbations associated with the event $D_n(k)$. Given data $D(k)$ similar to that of Figure 7, then, the linear data equations become

$$\alpha_{11}(-2k) + \alpha_{12}(-2k) - 2F(k)[\beta_{11}(-2k) + \beta_{12}(-2k)] = 4\frac{D(k)}{i2k}. \tag{50}$$

Using the assumption of step-like interfaces again, and placing these interfaces at pseudo-depth (i.e. imaging with c_0), we make the substitutions

$$
\begin{aligned}
\alpha_{11}(-2k) &= \alpha_{11}\frac{e^{i2kz_1}}{i2k},\\
\beta_{11}(-2k) &= \beta_{11}\frac{e^{i2kz_1}}{i2k},\\
\alpha_{12}(-2k) &= \alpha_{12}\frac{e^{i2kz_1}e^{i2k(z_2-z_1)}}{i2k},\\
\beta_{12}(-2k) &= \beta_{12}\frac{e^{i2kz_1}e^{i2k(z_2-z_1)}}{i2k}.
\end{aligned}
\tag{51}
$$

Then equations (48) and (50) combine to become

$$
\alpha_{11} - 2\beta_{11}F(k) + e^{i2k(z_2-z_1)}[\alpha_{12} - 2\beta_{11}F(k)] = 4R_1(k) + 4\tilde{R}_2(k)e^{i2k(z_2-z_1)}. \tag{52}
$$

From here we may proceed in two different ways. First, we may re-write this relationship as

$$
\alpha_{11} + L_1(k)\beta_{11} + L_2(k)\alpha_{12} + L_3(k)\beta_{11} = \hat{R}(k), \tag{53}
$$

where

$$
\begin{aligned}
L_1(k) &= -2F(k),\\
L_2(k) &= e^{i2k(z_2-z_1)},\\
L_3(k) &= L_1(k)L_2(k),\\
\hat{R}(k) &= 4R_1(k) + 4\tilde{R}_2(k)e^{i2k(z_2-z_1)},
\end{aligned}
\tag{54}
$$

and recognize that this constitutes an independent system of linear equations (since $L_n(k)$ are known and – usually – differ as k differs) which is overdetermined given greater than four input wavenumbers k. This procedure generalizes immediately to > 2 interfaces, with the caveats (a) larger numbers of input frequencies are required for larger numbers of interfaces, and (b) if events are close to one another such that $z_{n+1} - z_n \approx 0$, the procedure becomes less well-posed.

Secondly, if we can gain access to the local frequency content of each reflected event, i.e. if we can individually estimate $R_1(k)$, $\tilde{R}_2(k)$, etc., then, equating like pseudo-depths in equation (52), we have

$$
\begin{aligned}
\alpha_{11} - 2\beta_{11}F(k) &= 4R_1(k),\\
\alpha_{12} - 2\beta_{12}F(k) &= 4\tilde{R}_2(k).
\end{aligned}
\tag{55}
$$

This procedure also immediately generalizes to multiple interfaces, and is therefore a highly specific (in the sense of experimental configuration) approach to "interval Q estimation". It does not require large numbers of available frequencies as input, regardless of the number of interfaces, but it does require the adequate estimation of $\tilde{R}_2(k)$ and any subsequent deeper event $\tilde{R}_n(k)$.

We now proceed to demonstrate the latter interval Q estimation approach for two simple models (because of passing interest in this exact problem, and abiding interest in more general cases, e.g. two-parameter with offset, which we expect to behave similarly). Table 2 details the parameters used.

Model #	*Layer 1 c (m/s)*	*Layer 1 Q*	*Layer 2 c (m/s)*	*Layer 2 Q*
1	1550	200	1600	10
2	1550	100	1600	10

Table 2: *Test models used for the single layer c, Q linear inversion. The reference medium, $z < 500m$, is acoustic and characterized by $c_0 = 1500m/s$.*

Figures 8 – 9 illustrate the inversion for interval c/Q inversion on input data from models 1–2 using low-valued pairs of input frequencies. Figures 10 – 11 illustrate the inversion of the same two models, this time using two high-frequency input reflection coefficients.

Observing the progression of Figures 8 – 9, in which the layer Q becomes smaller (and attenuation increases), it is clear that the effective transmission effects of the viscoacoustic medium cause increasing error in the inversion for the lower medium. This is a natural part of linear viscoacoustic inversion, and stands as an indication that the raw estimate of absorptive/dispersive V_1 has limited value. However, comparing the same inversions using different input frequencies (i.e. Figures 10 – 11 compared to Figures 8 – 9), we also see that the inversion accuracy is dependent on which frequencies are utilized. At low frequency the effects of a viscous overburden negatively affect the inversion results, but the error is much smaller than at high.

To summarize, we may pose the 1D normal incidence two-parameter problem such that (assuming we have access to the reflection coefficients – with transmission error – $\widetilde{R}_n(k)$) a two-interface case may be handled. This means we may again take advantage of the simplicity of this surrogate version of the two-parameter with offset problem. We straightforwardly illustrate the increased transmission error associated with viscous propagation, but point out that the error is strongly dependent on which frequencies are used as input. Let us next take a closer look at this issue.

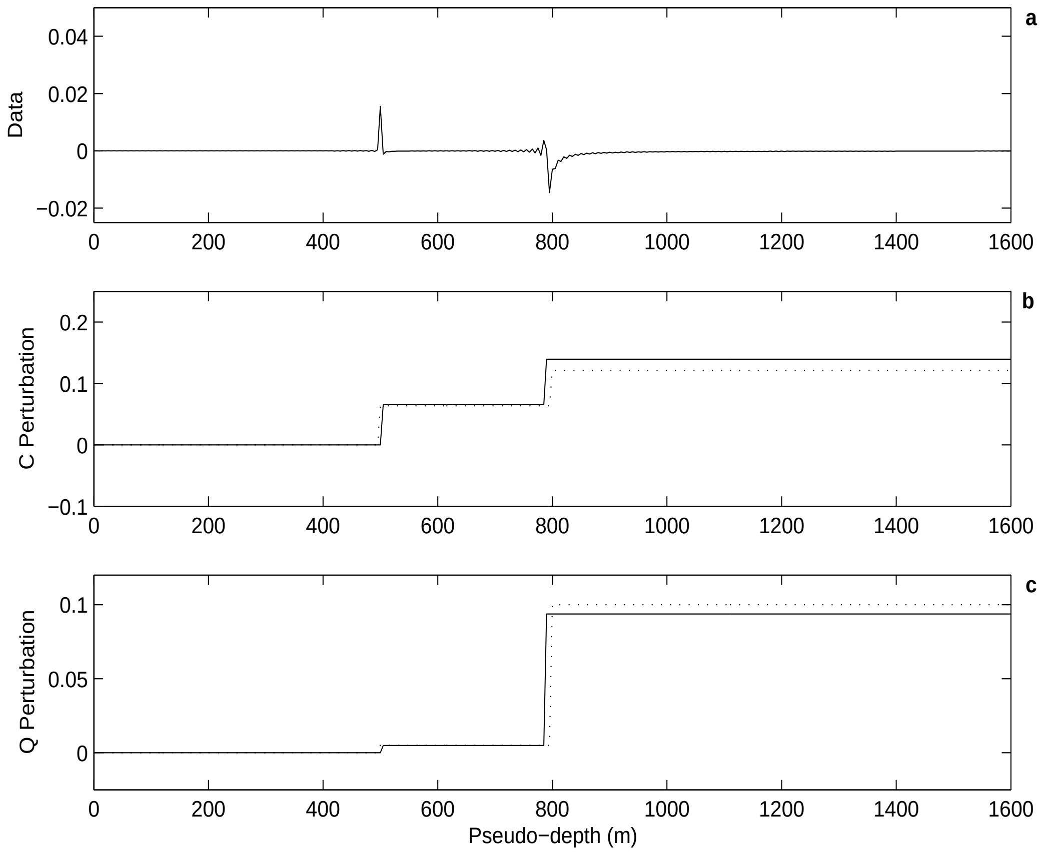

Figure 8: *Linear c, Q profile inversion for a single layer model (Model* 1 *in Table 2). (a) Data used in inversion plotted against pseudo-depth* $z = c_0t/2$*. (b) Recovered wavespeed perturbation* $\alpha_1(z)$ *(solid) plotted against true perturbation (dotted). (c) Recovered Q perturbation* $\beta_1(z)$ *(solid) against true perturbation (dotted). Low input frequencies used.*

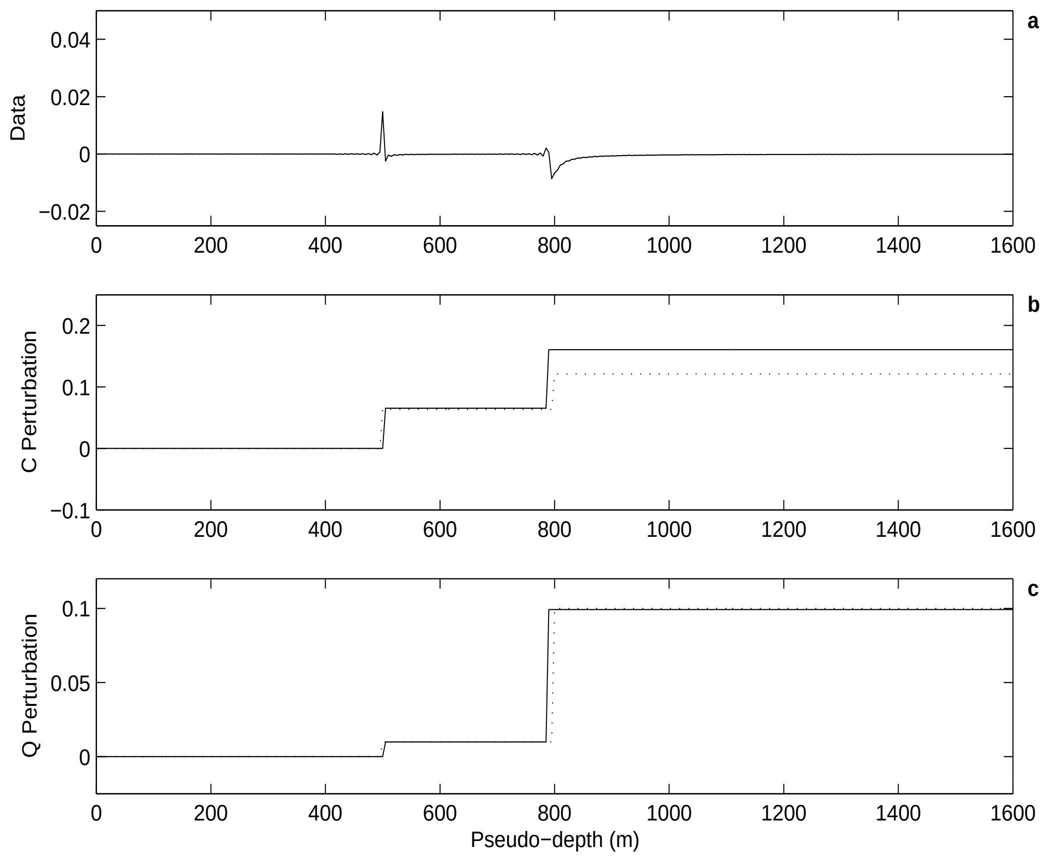

Figure 9: *Linear c, Q profile inversion for a single layer model (Model 2 in Table 2). (a) Data used in inversion plotted against pseudo-depth $z = c_0t/2$. (b) Recovered wavespeed perturbation $\alpha_1(z)$ (solid) plotted against true perturbation (dotted). (c) Recovered Q perturbation $\beta_1(z)$ (solid) against true perturbation (dotted). Low input frequencies used.*

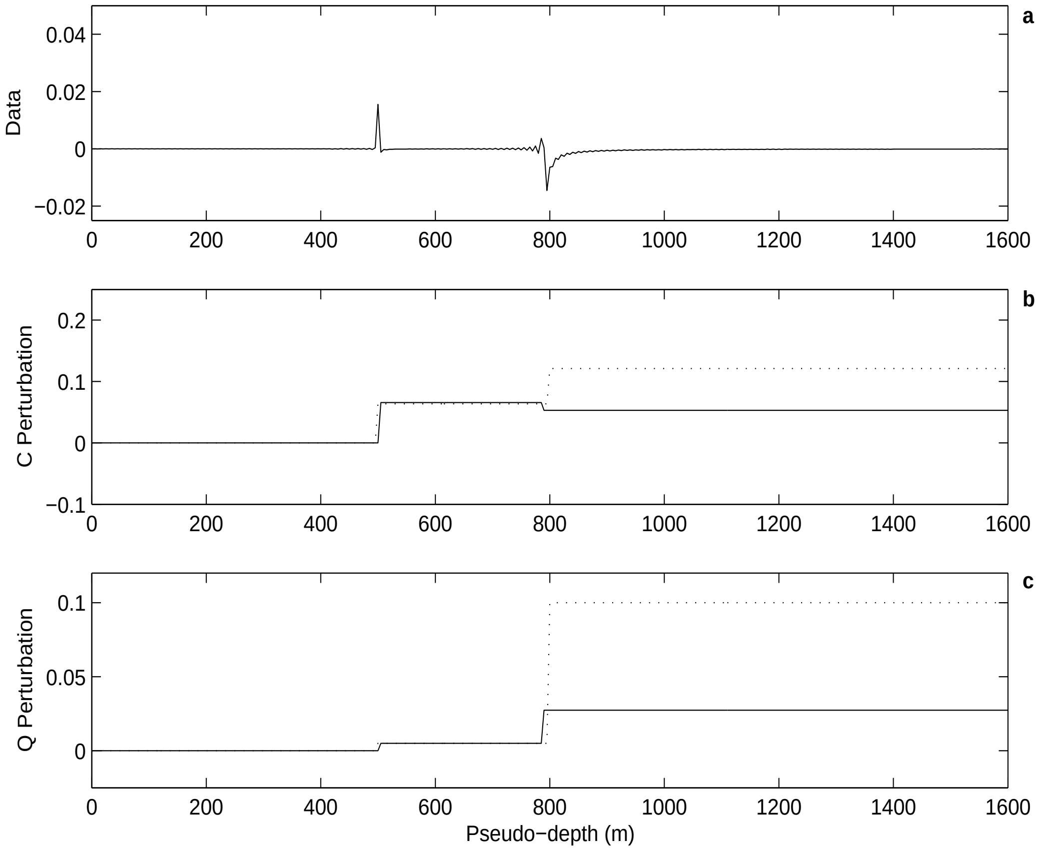

Figure 10: *Linear c, Q profile inversion for a single layer model (Model* 1 *in Table 2). (a) Data used in inversion plotted against pseudo-depth* $z = c_0 t/2$*. (b) Recovered wavespeed perturbation* $\alpha_1(z)$ *(solid) plotted against true perturbation (dotted). (c) Recovered Q perturbation* $\beta_1(z)$ *(solid) against true perturbation (dotted). High input frequencies used.*

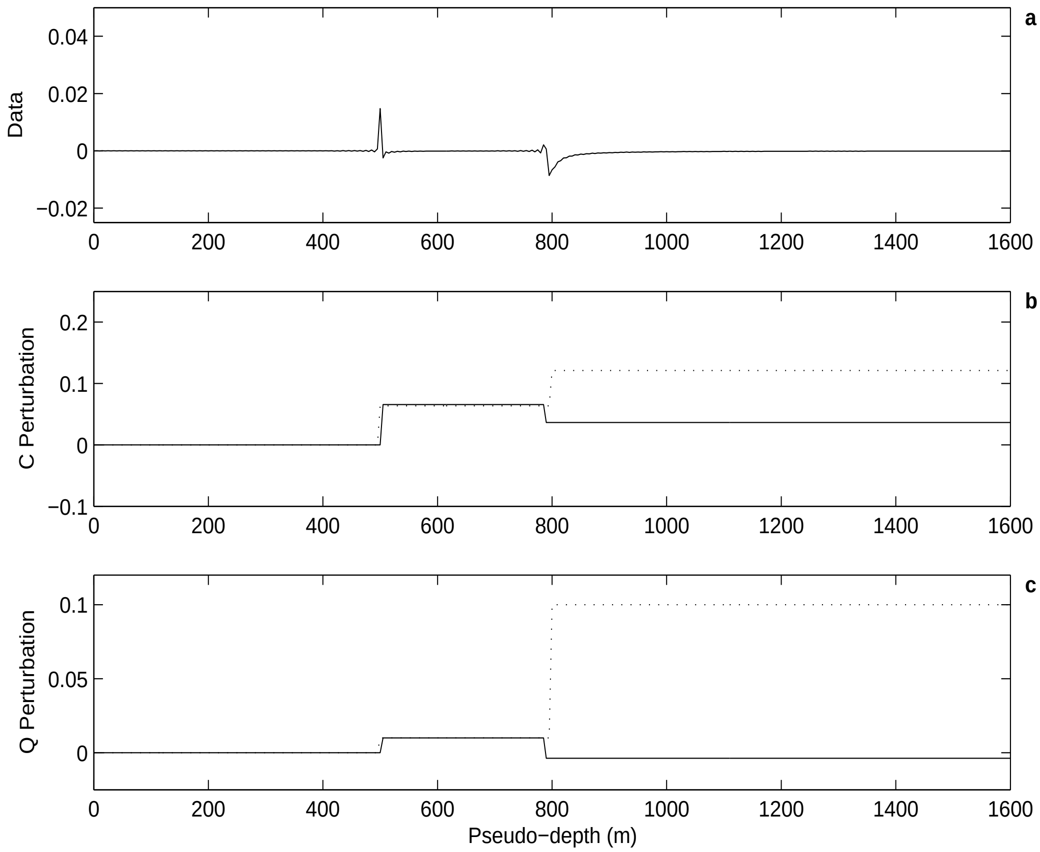

Figure 11: *Linear c, Q profile inversion for a single layer model (Model 2 in Table 2). (a) Data used in inversion plotted against pseudo-depth $z = c_0t/2$. (b) Recovered wavespeed perturbation $\alpha_1(z)$ (solid) plotted against true perturbation (dotted). (c) Recovered Q perturbation $\beta_1(z)$ (solid) against true perturbation (dotted). High input frequencies used.*

5.3 The Relationship Between *Accuracy* and *Frequency*

The examples of the previous section highlight an inherent source of inaccuracy in the linear inverse output of the absorptive/dispersive problem, namely that the attenuated reflection coefficients lead to parameter estimates that are often greatly in error. In the following section we will consider courses of action we may take to address this problem; here we will simply observe more closely one aspect of the nature of the viscoacoustic linear inverse problem, that may suggest strategies for minimizing the effect of attenuation on the linear result.

We have considered the "1D normal incidence + structural assumptions" problem as a simple surrogate for the "1D + offset" problem. In doing so we are able to cast a two-parameter estimation procedure as an overdetermined system of linear equations to be solved, with one equation/two unknowns for every frequency in the experiment. In the interval Q problem, having chosen two frequencies (and perfect data), we find that as soon as the lower event is significantly attenuated (i.e. the layer Q is strong enough) the Q estimate for the lower medium is deflected far from the true value. However, the deflection is not uniform for input frequency pairs. In this section we more closely consider the input frequencies used.

We apply the procedures of the two event interval Q problem to the sequence of input models/data sets described in Table 3. In this case we consider the output as a function of all possible input frequency pairs, which, similarly to the single-interface case, are plotted as surfaces against these pairs k_1, k_2. See Figures 12 – 16.

Observing the evolution of Q estimates for the upper and lower interfaces, a similar but slightly more complete picture is formed. Clearly as Q_1 becomes lower, and so the input reflection coefficient from the lower interface becomes more and more attenuated, the Q estimates become worse and worse. It is interesting to note, however, that the deflection of $Q_2(k_1, k_2)$ away from the true Q_2 is not uniform across frequency/wavenumber pairs. Rather, there is a tendency for the error to increase with higher frequencies. This is an intuitive result, since by its nature the attenuative medium saps the wave field (and therefore the effective reflection coefficient) of energy preferentially at the high frequencies.

It may eventually be profitable to include such insight into the choice of *weighting scheme* that will be part of the solution of the overdetermined systems, weighting more heavily the contributions from lower frequency pairs. In the analogous "1D with offset" problem this will amount to a judicious weighting of angle, or offset, contributions in the estimation, rather than explicitly frequency contributions.

Model #	*Layer 1 c (m/s)*	*Layer 1 Q*	*Layer 2 c (m/s)*	*Layer 2 Q*
1	1550	300	1600	10
2	1550	250	1600	10
3	1550	200	1600	10
4	1550	150	1600	10
5	1550	100	1600	10

Table 3: *Test models used for the single layer c, Q linear inversion. The reference medium, $z < 500m$, is acoustic and characterized by $c_0 = 1500m/s$.*

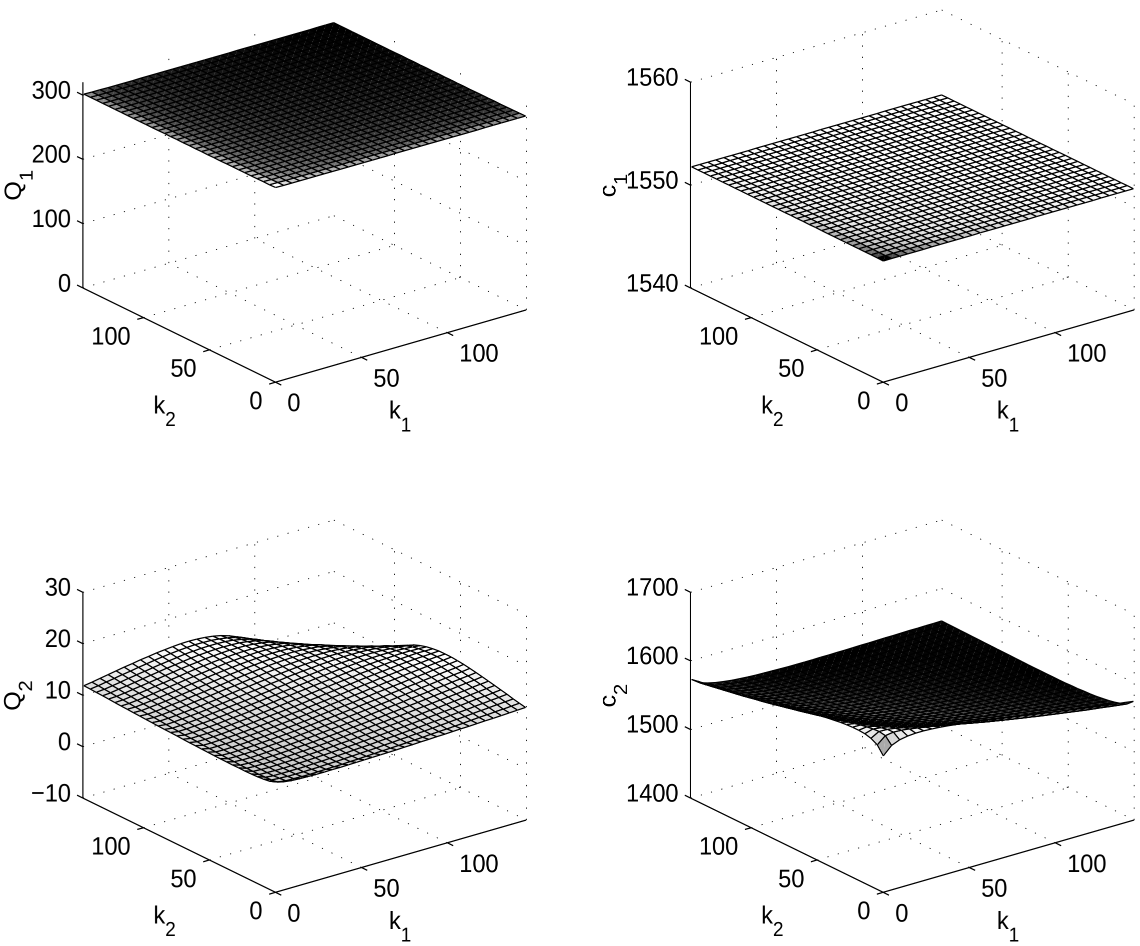

Figure 12: *Linear c, Q profile inversion for a single layer model (Model 1 in Table 3). Top left: Q estimate for top interface; top right: wavespeed estimate for top interface; bottom left: Q estimate for lower interface; bottom right: wavespeed estimate for lower interface. Frequencies (denoted k_1 and k_2) are in units of Hz.*

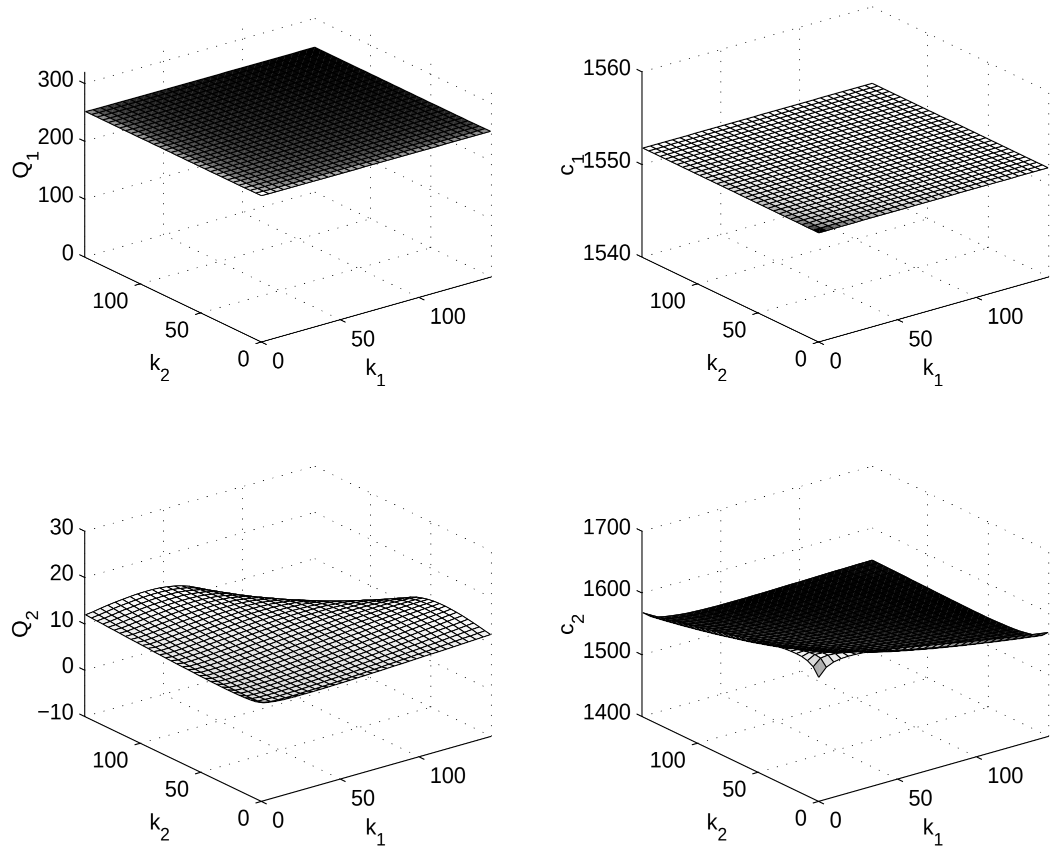

Figure 13*: Linear c, Q profile inversion for a single layer model (Model* 2 *in Table 3). Top left: Q estimate for top interface; top right: wavespeed estimate for top interface; bottom left: Q estimate for lower interface; bottom right: wavespeed estimate for lower interface. Frequencies (denoted k_1 and k_2) are in units of Hz.*

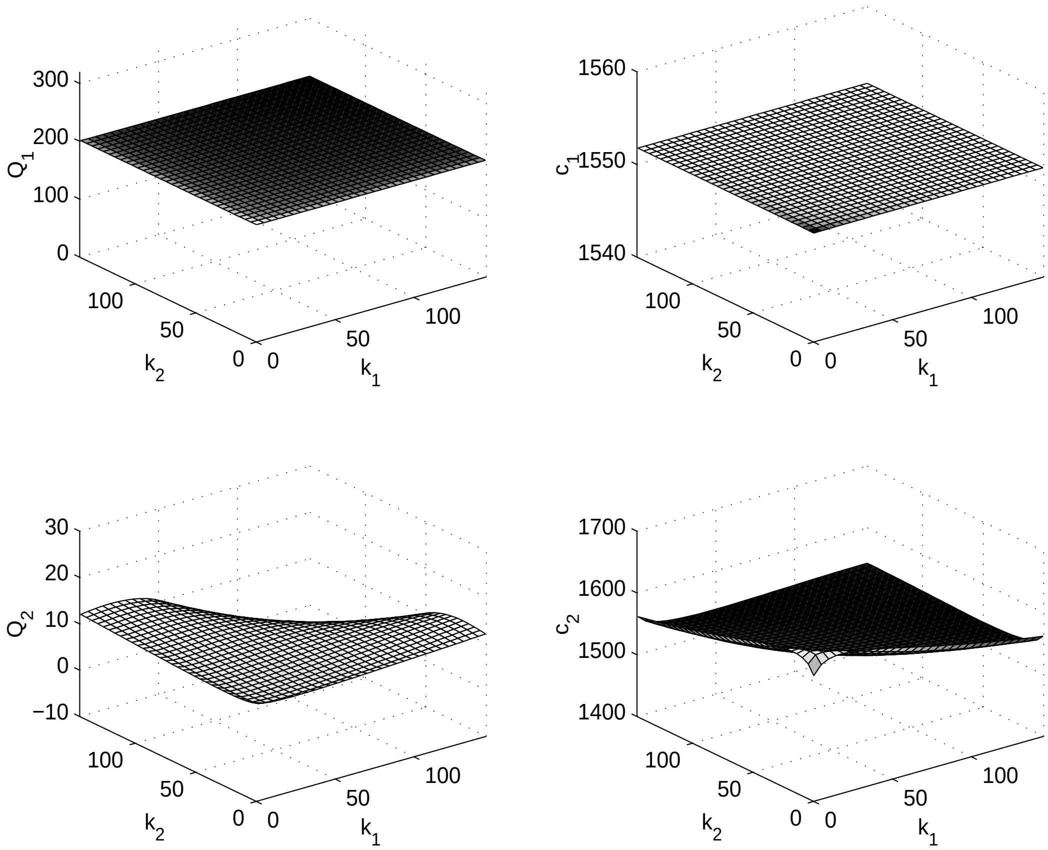

Figure 14*: Linear c, Q profile inversion for a single layer model (Model* 3 *in Table 3). Top left: Q estimate for top interface; top right: wavespeed estimate for top interface; bottom left: Q estimate for lower interface; bottom right: wavespeed estimate for lower interface. Frequencies (denoted* k_1 *and* k_2*) are in units of Hz.*

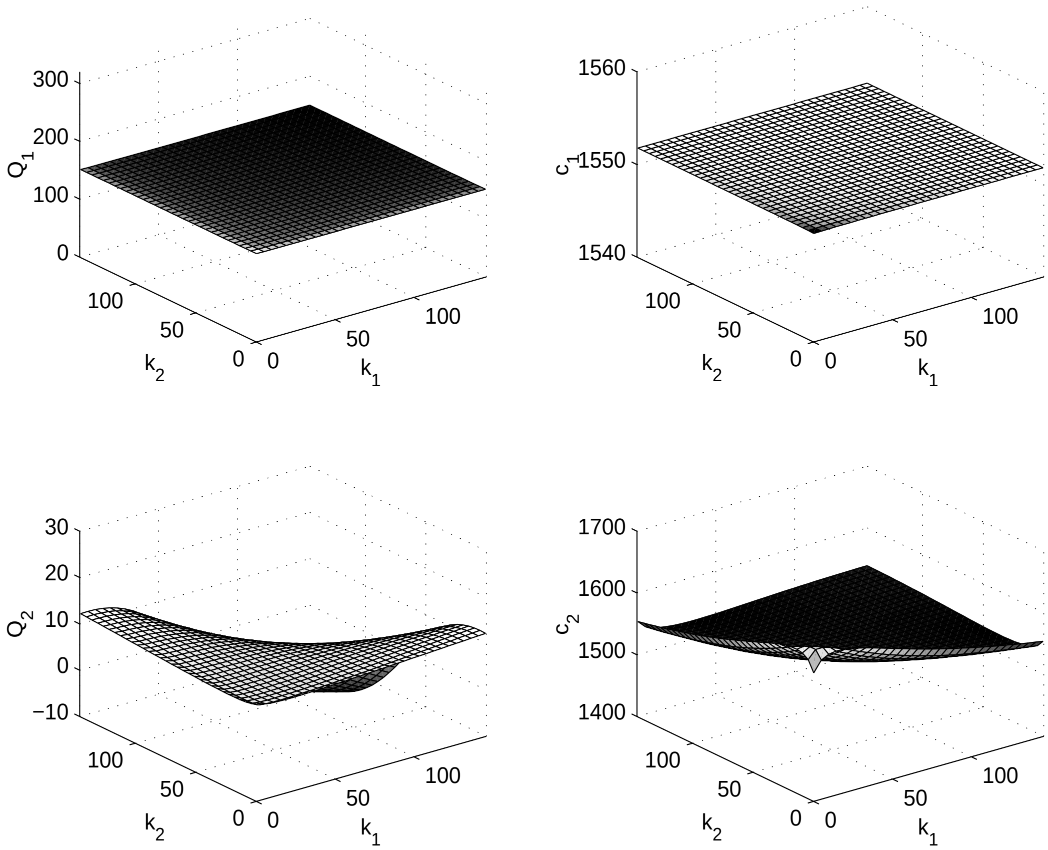

Figure 15*: Linear c, Q profile inversion for a single layer model (Model* 4 *in Table 3). Top left: Q estimate for top interface; top right: wavespeed estimate for top interface; bottom left: Q estimate for lower interface; bottom right: wavespeed estimate for lower interface. Frequencies (denoted k_1 and k_2) are in units of Hz.*

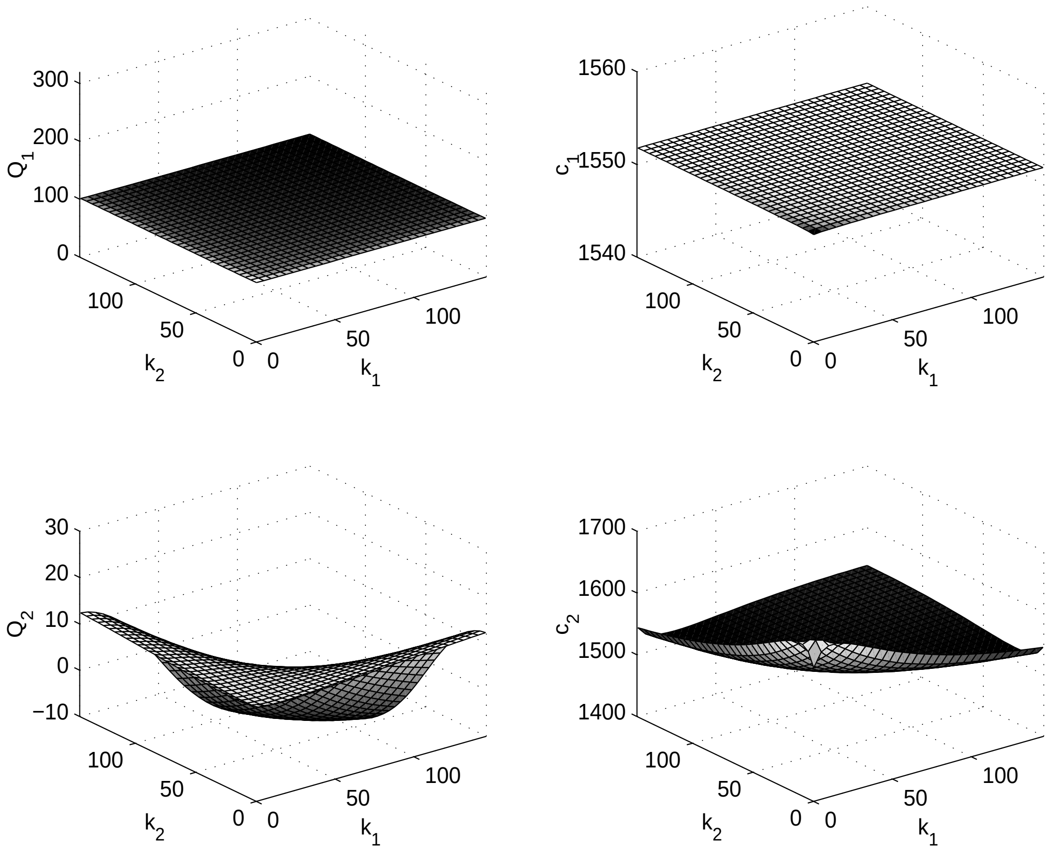

Figure 16*: Linear c, Q profile inversion for a single layer model (Model* 5 *in Table 3). Top left: Q estimate for top interface; top right: wavespeed estimate for top interface; bottom left: Q estimate for lower interface; bottom right: wavespeed estimate for lower interface. Frequencies (denoted* k_1 *and* k_2*) are in units of Hz.*

5.4 A Layer-stripping Correction to Linear Q Estimation

There are two proactive ways we could attempt to rectify the problem of decay of reflectivity: (1) correct the linear result with an ad hoc patch, or (2) resort to nonlinear methodologies, since viscoacoustic propagation is a nonlinear effect of the medium parameters on the wave field (Innanen, 2003; Innanen and Weglein, 2003).

The latter approach is material for a subsequent report. For now, we illustrate a correction to the linear inverse results that amounts to a layer stripping strategy. Using the local-reflectivity approach of the previous section, recall that we solved for amplitudes of step-like contrasts α_{1n}, β_{1n} via effective reflection coefficients (equation (51)). In general, the equations are

$$
\begin{aligned}
&\alpha_{11} - 2\beta_{11}F(k) = 4R_1(k),\\
&\alpha_{12} - 2\beta_{12}F(k) = 4\tilde{R}_2(k),\\
&\alpha_{13} - 2\beta_{13}F(k) = 4\tilde{R}_3(k),\\
&\vdots\\
&\alpha_{1N} - 2\beta_{1N}F(k) = 4\tilde{R}_N(k),
\end{aligned}
\tag{56}
$$

where

$$
\tilde{R}_N(k) = R'_N(k)\exp\left\{\sum_{j=1}^{N} i2\left[\frac{\omega}{c_{j-1}}\frac{F(k)}{Q_{j-1}}\right](z'_j - z'_{j-1})\right\}. \tag{57}
$$

In other words, the effective reflection coefficients in the data are the desired reflection coefficients (still in error by transmission from the overburden) operated on by an absorption/dispersion factor.

Implementing the low-contrast approximation $z'_j - z'_{j-1} \approx z_j - z_{j-1}$, and recognizing that the first step is to estimate c_1 and Q_1 from the unaffected reflection coefficient $R_1(k)$, we can apply a corrective operator to the next lowest reflection coefficient:

$$
R'_2(k) \approx \frac{\tilde{R}_2(k)}{\exp[i2\frac{\omega}{c_1}\frac{F(k)}{Q_1}(z_2 - z_1)]}. \tag{58}
$$

This approximation is closer to that which equations (56) “would like to see”, a reflection coefficient with attenuation corrected-for. This may be done for deeper events also, making use of equation (57) to design appropriate corrective operators.

Figures 17 – 18 demonstrate the use of this layer stripping, or “bootstrap”, approach to patching up the linearized interval Q estimation procedure for mid range input frequencies; the models used are detailed in Table 2. Clearly the results are far superior, and there is reason to be encouraged by this approach. A note of caution: the estimated Q values are in error by a small amount due to the linear approximation, so each correction of the next deeper reflection coefficient will be in increasing error. Q-compensation of this kind is sensitive to input Q values, so one might expect the approach to eventually succumb to cumulative error.

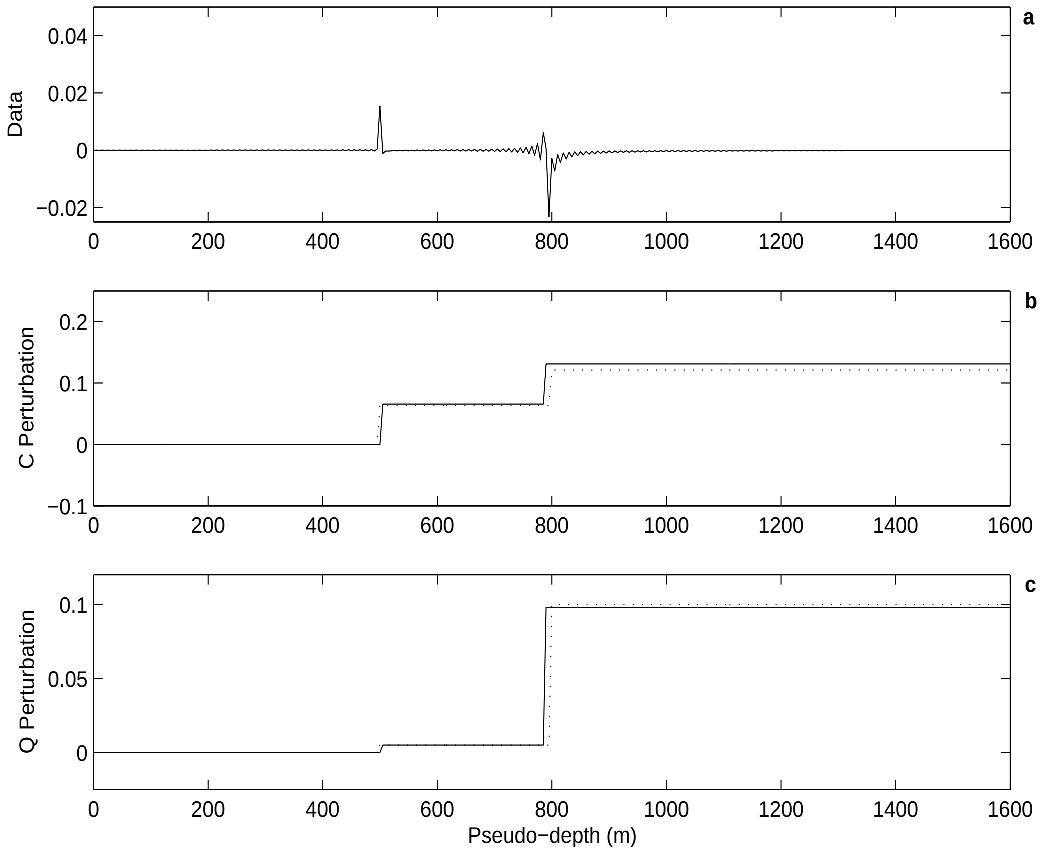

Figure 17*: Linear c, Q profile inversion for Model* 1 *in Table 2 with attenuative propagation effects compensated for. (a) Data used in inversion plotted against pseudo-depth $z = c_0t/2$. (b) Recovered wavespeed perturbation $\alpha_1(z)$ (solid) plotted against true perturbation (dotted). (c) Recovered Q perturbation $\beta_1(z)$ (solid) against true perturbation (dotted).*

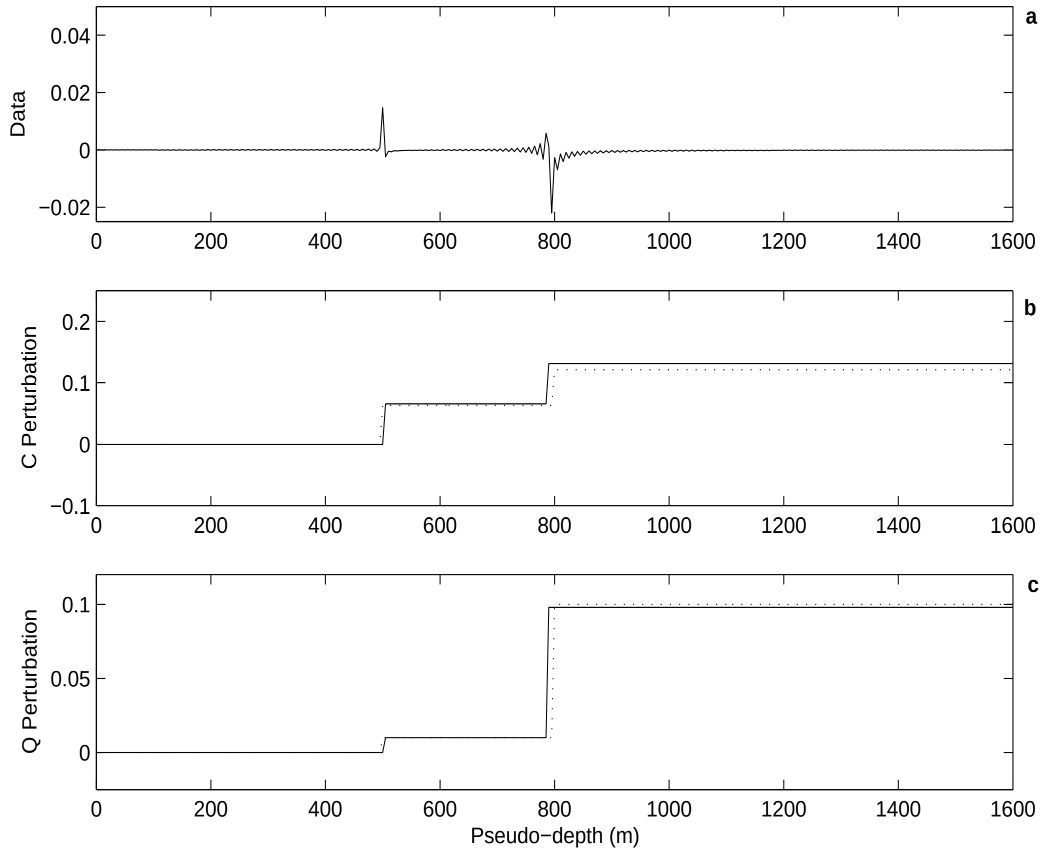

Figure 18: *Linear c, Q profile inversion for Model* 2 *in Table 2 with attenuative propagation effects compensated for. (a) Data used in inversion plotted against pseudo-depth* $z = c_0 t/2$. *(b) Recovered wavespeed perturbation* $\alpha_1(z)$ *(solid) plotted against true perturbation (dotted). (c) Recovered Q perturbation* $\beta_1(z)$ *(solid) against true perturbation (dotted).*

6 Conclusions

We have demonstrated some elements of a linear Born inversion for wavespeed and Q with arbitrary variation in depth. The development generates a well-posed (overdetermined) estimation scheme for arbitrary distributions two parameters in depth, given shot record-like data. The nature of this viscoacoustic inversion is such that a 1D normal incidence version of the problem can be made tractable (and in many ways comparable to the general problem) for two parameters with the assumption of a basic structural form for the model. The simplicity of this casting of the problem makes it useful as a way to develop the basics of the linear viscoacoustic inversion problem.

For a single interface, accuracy is high up to very large Q contrast, with the caveat that the required input to this inversion are the rather subtle spectral properties of the absorptive/dispersive reflection coefficient. For interval c/Q estimation, the attenuation of the reflected events (a process that is nonlinear in the parameters) produces exaggerated transmission error in the estimation; we show that this is mitigated by both judicious choice (or weighting) of input frequencies and/or an ad hoc bootstrap/layer-stripping type correction of lower reflection coefficients.

We develop this linear estimation procedure for two reasons – first in an attempt to produce useful linear Q estimates, and second because this estimate (or something very like it) is the main ingredient for a more sophisticated nonlinear inverse scattering series procedure. Results are encouraging on both fronts.

Acknowledgments

The authors thank the sponsors and members of M-OSRP and CDSST, especially Simon Shaw, Bogdan Nita and Tad Ulrych, for discussion and support.

References

Aki, K. and Richards, P. G. "Quantitative Seismology." *University Science Books*, (2002): 2nd Ed.

Born, M. and Wolf, E. "Principles of Optics." *Cambridge University Press*, (1999): 7th Ed.

Clayton, R. W. and Stolt, R. H. "A Born-WKBJ Inversion Method for Acoustic Reflection Data." *Geophysics 46*, (1981):1559.

Cohen, J. K. and Bleistein, N. "An Inverse Method for Determining Small Variations in Propagation Speed." *SIAM Journal of Applied Math 32*, (1977):784–799.

Dasgupta, R. and Clark, R. A. "Estimation of Q From Surface Seismic Reflection Data." *Geophysics 63*, (1998):2120–2128.

Innanen, K. A. "Methods for the Treatment of Acoustic and Absorptive/Dispersive Wave Field Measurements." *Ph.D. Thesis, University of British Columbia*, (2003).

Innanen, K. A. and Weglein, A. B., "Construction of Absorptive/Dispersive Wave Fields with the Forward Scattering Series." *Journal of Seismic Exploration*, (2003): In Press.

Kjartansson, E. "Constant-Q Wave Propagation and Attenuation." *Journal of Geophysical Research 84*, (1979):4737–4748.

Raz, S. "Direct Reconstruction of Velocity and Density Profiles from Scattered Field Data." *Geophysics 46*, (1981):832.

Tonn, R. "The Determination of the Seismic Quality Factor Q from VSP Data: a Comparison of Different Computational Methods." *Geophysical Prospecting 39*, (1991):1–27.

Weglein, A. B. "The Inverse Scattering Concept and its Seismic Application." *In: Dev. in Geophys. Explor. Meth., Fitch, A. A. Ed. 6*, (1985):111–138.